FLIGHT DYNAMICS ANALYSIS AND BASIC STABILIZATION STUDY IN EARLY DESIGN STAGES OF THE SAGITTA DEMONSTRATOR UAV

M. Geiser and M. Heller

Institute for Advanced Study, Technische Universität München
Lichtenbergstrasse 2a, D-85748 Garching, Germany

Abstract

This paper addresses the flight dynamics modelling and analysis as well as the basic stabilization study of the *SAGITTA Demonstrator* in early design stages. A focus is to support the process of control effectors specification with trim, maneuvering and stabilization requirements to reduce the count of design iterations.

The *SAGITTA Demonstrator*, flying testbed of the open innovation project *SAGITTA*, represents a flying wing configuration, which is characterized by (static) lateral-directional instability in regions of its flight envelope.

Regarding the trim curve analysis, it is common practice to investigate the target flight envelope for regions where it is not possible to trim the aircraft due to limited control power. Without the control effectors being specified, the evaluation of the trimmability has to be replaced by the derivation of least control moment needs ensuring trimmability.

Besides the mere ability to trim the aircraft in different mission relevant flight conditions, every aircraft has to meet requirements regarding its dynamic charcteristics. For manned aircraft, these requirements are usually derived from the need to guarantee a certain level of flying and handling qualities. In case of autonomous unmanned systems, handling qualities are less relevant but instead requirements driven by the designated mission and hence the maneuver performance come to the fore. In this context, a lower bound for the needed roll control effectiveness to achieve a desired steady state bank angle within a given time will be derived analytically.

Typically, an assessment of the stabilization capability is conducted in case of an inherent unstable design by means of nonlinear simulation after control effectors and control laws have (preliminary) been specified. This bears the risk of an undesirable high count of design iterations until an adequate trade-off between the degree of instability and the superior design objectives (as performance, low observability, etc.) will be achieved. In contrast to that approach, a basic stabilization study is accomplished prior to the specification of control effectors or control laws. This study applies a novel methodology balancing the destabilizing moment build-up due to a sideslip disturbance independently against the counteracting control moment development in terms of a worst case approximation of the real effective moment build-up of a controlled aircraft.

1. INTRODUCTION

In the year 2011, the open innovation project *SAGITTA* was launched as a joint research program of German universities, research facilities and the industry partner *CASSIDIAN*. Thereby *SAGITTA* aims at identifying and closing technology gaps for the development of future unmanned aerial vehicle (UAV) systems through fundamental research and validation of its results by application to a scaled flying testbed, the so-called *SAGITTA Demonstrator*, which is depicted in FIGURE 1.

The *SAGITTA Demonstrator* represents a flying wing configuration without vertical stabilizers, which is characterized by (static) lateral-directional instability in regions of its flight envelope. For this reason, controller based stabilization is required and an assessment of the stabilization capability is mandatory already in early steps of the design process.

As indicated within FIGURE 1, a *Clean Side* and a so-called *Dirty Side* have been specified for the flying wing. While the landing gear as well as inlets and nozzles of the propulsion system are located on the *Dirty Side*, there are no openings on the *Clean Side*. This shall support the low observability concept and requires the ability to fly with the *Clean Side* pointing up, e.g. for start and landing, as well as with the *Dirty Side* pointing up to display the low observable *Clean Side* to the ground.

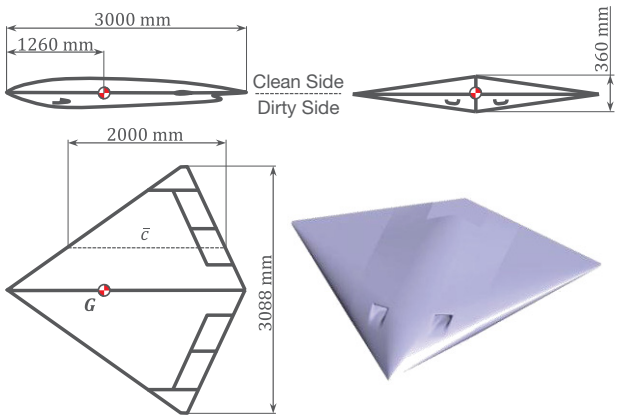

FIGURE 1: Sketch of the *SAGITTA Demonstrator*

2. FLIGHT DYNAMICS MODELLING

Mathematical models of the aircraft in its environment are among others required for analyses of the trimmability and the stabilization capability as well as for design and assessment of control laws.

The complexity of the applied models significantly depends on the task to be fulfilled. For instance, control law design is often performed based on linearized representations of the aircraft's dynamics while control law assessment usually has to be accomplished utilizing a nonlinear six degrees of freedom (6-DoF) model.
In this connection, the less complex models are typically derived from the nonlinear 6-DoF model, e.g. by means of linearization w.r.t. trim points, and hence only one master model has to be implemented and actively kept up to date during the design process.
Frequently, most of the framework of such a master model is available before the actual design process starts. The geophysics as well as the nonlinear rigid-body equations of motion are for example completely independent of the plant to be modelled and the aircraft specific flight mechanics model, including amongst others the aerodynamics, is at least similar in its structure for most configurations.
Once the configuration details have been specified, it is sufficient to apply the data to the prepared master model and to extend or adopt its framework where necessary.
In early design stages however, only limited data of the aircraft is available and hence the finalization of the nonlinear 6-DoF model is not necessarily straightforward.
Often, in particular prior to the so-called design freeze, it is required to apply simplifications to the 6-DoF model since the actual properties are subject to open design decisions.
With good knowledge of the derivation of lower complexity models, it is possible to propagate the effects of respective simplifications analytically.
Alternatively, if a model of lower complexity with a small number of not yet specified parameters is applied for an analysis, it can be rewarding to utilize the analytic model in its parametric form and determine limits for the free parameters such that certain requirements are satisfied.

In case of the *SAGITTA Demonstrator*, the control effectors should be tailored to meet a set of flight dynamics requirements. Hence, configuration analyses had to identify the needed control effectiveness and the respective dynamics as input for the controls design. For this, model simplifications as well as analytic models of lower complexity have been applied.
For the determination of the control effectiveness demand for trimmability, the control effectors were modelled as three generic moment sources, providing a decoupled rolling, pitching and yawing moment respectively, without effect on the aircraft's force balance.
With innovative controls concepts conceivable, this approach without presumptions regarding the realization of the control moments was advantageous over exemplary textbook flap models approximating standard control surfaces since the actual dimensioning parameter of the control effectors could be determined.
A further control effectiveness demand to provide a certain roll performance could be determined to some extent analytically with linearized lateral dynamics.

As soon as a controls concept was specified, the corresponding models have been extended in order to account for known couplings and interdependencies.

3. FLIGHT DYNAMICS ANALYSIS

During the aircraft design process, flight dynamics analyses are performed repeatedly on different levels of complexity and with a different focus.
Some of these analyses are based on rather simple models and are primarily applied in very early design stages.
Others are relevant over the whole design process and gain significance with the continuously improving models.
Especially for the latter type of analyses, a high level of automation is reasonable. However, the final interpretation of the generated data is always a major duty of the flight dynamics engineer.

In case of the *SAGITTA Demonstrator*, the foundations for the control effectors design process shall be provided by means of flight dynamics analysis. For this purpose, the control demands for trimming plus maneuvering as well as stabilization and / or the modification of flying qualities have to be determined.
Although several of these control demands have to be satisfied overlaying, i.e. accumulating, it is reasonable to summarize only those that may actually occur together in order not to be too conservative with the controls concept.
If e.g. roll performance requirements do not have to be satisfied in a flight with steady heading sideslip and one engine inoperative, there is no need to superimpose the control demands of a corresponding trim condition and the rolling maneuver. Respective exceptions have to be introduced to the automated assessment routines according to the performance specifications.
The control demand for an augmentation of the dynamics on the other hand is always on top of trimming and maneuvering. Unfortunately, this type of control demand is hard to determine in early design stages since the augmentation system has typically not yet been designed. Due to this limitation, it is only possible to give a conservative but convenient approximation of the control demand for augmentation via a basic stabilization study.

The following sections give further details on the trim curve analysis and on the analysis of the roll performance as an example for the derivation of maneuvering requirements.
The assessment of the UAV's stabilization capability and derived requirements for the control effectors will be addressed in Section 4 by means of the basic stabilization study.
For analyses primarily dealing with the inherent dynamics of the zero controls configuration, e.g. the assessment of the speed stability and the maneuver stability or evaluations of the eigenmodes, it shall be referred to [1].

3.1. Trim Curve Analysis

Regarding the trim curve analysis, it is common practice to investigate the target flight envelope for regions where it is not possible to trim the aircraft due to limited control power.
Without control effectors being specified, the evaluation of the trimmability has to be replaced by the derivation of least control moment needs ensuring trimmability.
These control requirements are expressed in terms of the necessary increments to the pitching, rolling and yawing moment coefficient via the generic moment sources described in Section 2 to trim the aircraft.
Representative trim curves for the derivation of control requirements in the longitudinal motion can be gained

from the steady-state wings-level flight and the symmetric quasi-steady pull up / push over maneuver.
In the lateral motion, the focus is set on the coordinated turn as well as straight flight with steady sideslip, i.e. steady heading sideslip. Here, the latter is not meant for operational purpose but shall approximate the control demand of the decrab maneuver just before a landing under cross-wind conditions. In this context, also scenarios with one engine inoperative have to be considered for our UAV equipped with two jet engines.

The overall control requirements for trimmability of the UAV correspond to the maximum control requirements of the applicable trim curves.
Limitations in applicability can result from restrictions of the aircraft's operational conditions. The steady heading sideslip trim curves for example are only relevant up to angles of sideslip that correspond at the evaluated airspeed to the limited cross-wind.

3.2. Roll Performance Analysis

Besides the mere ability to trim the aircraft in different mission relevant flight conditions, every aircraft has to meet requirements regarding its dynamic charcteristics. For manned aircraft, these requirements are usually derived from the need to guarantee a certain level of flying and handling qualities. In case of autonomous unmanned systems, handling qualities are less relevant but instead requirements driven by the designated mission and hence the maneuver performance come to the fore.

In this context, a lower bound for the needed roll control effectiveness to achieve a steady state bank angle of $\Phi = 180°$ within 2 seconds from a steady state bank angle of $\Phi = 0°$ will be derived analytically.
In order to prevent a significant curvature of the lateral flight path, the respective roll shall be performed along the aircraft's body fixed x_B-axis with an angle of attack $\alpha = 0°$, starting in a flat climbing flight, which reduces the loss of height during the maneuver.

For the subsequent analysis, we apply the assumption of decoupled longitudinal and lateral dynamics. Further it is assumed that the yaw rate r and the angle of sideslip β are kept constant at zero. For yaw controls with negligible effect on the rolling moment L, the aircraft's roll dynamics can be represented by the reduced state space model

$$\begin{bmatrix}\dot{p}\\ \dot{\Phi}\end{bmatrix} = \begin{bmatrix}L_p & 0\\ 1 & 0\end{bmatrix}\begin{bmatrix}p\\ \Phi\end{bmatrix} + \begin{bmatrix}L_\xi\\ 0\end{bmatrix}\xi \tag{1}$$

with the roll control input ξ and

$$\begin{aligned} L_p &\approx \frac{\bar{q}_0 S s C_{l,p}}{I_{xx}^G}\cdot\frac{s}{V_0} < 0\\ L_\xi &\approx \frac{\bar{q}_0 S s C_{l,\xi}}{I_{xx}^G} < 0 \end{aligned} \tag{2}$$

Referring to the state space model in Eqn.(1), the bank angle Φ is just an integration of the roll rate p while the dynamics of the roll rate itself are given by

$$\dot{p}(t) = L_p \cdot p(t) + L_\xi \cdot \xi(t) \tag{3}$$

Although the linearization was accomplished for p_0 and Φ_0 equal to zero, Eqn. (3) is also valid beyond this trim point and we can apply it for the subsequent derivations.

In the frequency domain, Eqn. (3) is represented by

$$p(s) = \frac{L_\xi}{s - L_p}\xi(s) + \frac{1}{s - L_p}p_0 \tag{4}$$

and for a step input $\xi(t) = \xi_0 \cdot \sigma(t)$, which corresponds to $\xi(s) = \xi_0/s$ in the frequency domain, it reads

$$p(s) = -\frac{L_\xi}{L_p}\cdot\frac{-L_p}{s(s - L_p)}\xi_0 + \frac{1}{s - L_p}p_0 \tag{5}$$

Here, the step input represents an ideal control effector and hence our final result will pose a lower bound of the roll control requirement.

Back in the time domain, Eqn. (5) is equivalent to

$$p(t) = -\frac{L_\xi}{L_p}\cdot(1 - e^{L_p t})\cdot\xi_0 + e^{L_p t}\cdot p_0 \tag{6}$$

and the following holds for the bank angle:

$$\begin{aligned} \Phi(t) &= \int_0^t p(\tau)d\tau\\ &= -\frac{L_\xi}{L_p}\cdot\left(t + \frac{1}{L_p}(1 - e^{L_p t})\right)\cdot\xi_0\\ &\quad -\frac{1}{L_p}(1 - e^{L_p t})\cdot p_0 + \Phi_0 \end{aligned} \tag{7}$$

With $L_p < 0$, it is obvious to see from Eqn. (6) that the roll rate p converges to a steady state roll rate

$$p_{SS} = -\frac{L_\xi}{L_p}\cdot\xi_0 \tag{8}$$

Although $p(t)$ actually never reaches p_{SS}, one typically assumes that $p(t) = p_{SS}$ for $t \geq 3 \cdot T_R$ for ideal 1st order dynamics, where T_R represents the roll time constant

$$T_R = -\frac{1}{L_p} \tag{9}$$

In the new notation, Eqns. (6) and (7) are given by

$$p(t) = \left(1 - e^{-t/T_R}\right)\cdot p_{SS} + e^{-t/T_R}\cdot p_0 \tag{10}$$

$$\begin{aligned} \Phi(t) &= \left(t - T_R\left(1 - e^{-t/T_R}\right)\right)\cdot p_{SS}\\ &\quad + T_R\left(1 - e^{-t/T_R}\right)\cdot p_0 + \Phi_0 \end{aligned} \tag{11}$$

Provided that we are only interested in $p(t)$ and $\Phi(t)$ for $t \geq 3 \cdot T_R$, it is justified to assume that p has reached the steady state roll rate p_{SS} and consequently the exponential functions in Eqn. (11) can be set to zero yielding

$$\Phi(t) = (t - T_R)\cdot p_{SS} + T_R \cdot p_0 + \Phi_0 \tag{12}$$

Without the exponential functions, we can conduct the analysis analytically and do not have to resort to numerical solvers.

For our roll maneuver starting in a steady state wings-level flight with $\Phi_0 = 0°$, Eqn. (12) reduces to the well-known approximation of the bank angle as an integration of p_{SS} over time, delayed by T_R:

$$\Phi(t) = (t - T_R)\cdot p_{SS} \tag{13}$$

It is straightforward to solve this equation for the time t_{SWITCH} required to obtain a certain bank angle Φ_{SWITCH}:

$$t_{SWITCH} = \frac{\Phi_{SWITCH}}{p_{SS}} + T_R \tag{14}$$

At time t_{SWITCH}, the aircraft still rolls at the rate p_{SS} and hence, a phase of deceleration back to p equal zero has to follow. Although the roll rate would already decay subject to the roll damping, ξ shall be switched step-like to the opposite value for maximum deceleration over the time interval Δt:

$$\begin{aligned} p(t_{\mathrm{SWITCH}} + \Delta t) &= -\left(1 - e^{-\Delta t/T_R}\right) \cdot p_{SS} \\ &\quad + e^{-\Delta t/T_R} \cdot p_{SS} \\ &= -\left(1 - 2e^{-\Delta t/T_R}\right) \cdot p_{SS} \end{aligned} \tag{15}$$

For a steady state level flight at $\Phi = \Phi_{STOP} = 180°$, the roll rate at the end of the deceleration phase has to be zero and hence Δt has to satisfy

$$1 - 2e^{-\Delta t/T_R} = 0 \tag{16}$$

Solved for Δt one gets

$$\Delta t = T_R \cdot \ln 2 \tag{17}$$

Consequently, with Eqn. (11) the bank angle change $\Delta\Phi$ over the deceleration phase is given by:

$$\begin{aligned} \Delta\Phi &= -\left(\Delta t - T_R\left(1 - e^{-\Delta t/T_R}\right)\right) \cdot p_{SS} \\ &\quad + T_R\left(1 - e^{-\Delta t/T_R}\right) \cdot p_{SS} \\ &= -\left(T_R \ln 2 - T_R\left(1 - \frac{1}{2}\right)\right) \cdot p_{SS} \\ &\quad + T_R\left(1 - \frac{1}{2}\right) \cdot p_{SS} \\ &= T_R \cdot (1 - \ln 2) \cdot p_{SS} \end{aligned} \tag{18}$$

With $\Delta\Phi = \Phi_{STOP} - \Phi_{SWITCH}$ at hand, t_{SWITCH} can be determined from Eqn. (14):

$$\begin{aligned} t_{SWITCH} &= \frac{\Phi_{STOP} - \Delta\Phi}{p_{SS}} + T_R \\ &= \frac{\Phi_{STOP}}{p_{SS}} + T_R \cdot \ln 2 \end{aligned} \tag{19}$$

The overall time $t_{\Phi,STOP}$ is then given by:

$$\begin{aligned} t_{\Phi,STOP} &= t_{SWITCH} + \Delta t \\ &= \frac{\Phi_{STOP}}{p_{SS}} + T_R \cdot \ln 4 \end{aligned} \tag{20}$$

Lines of constant t_{SWITCH} are depicted in FIGURE 2 over combinations of T_R and p_{SS}.

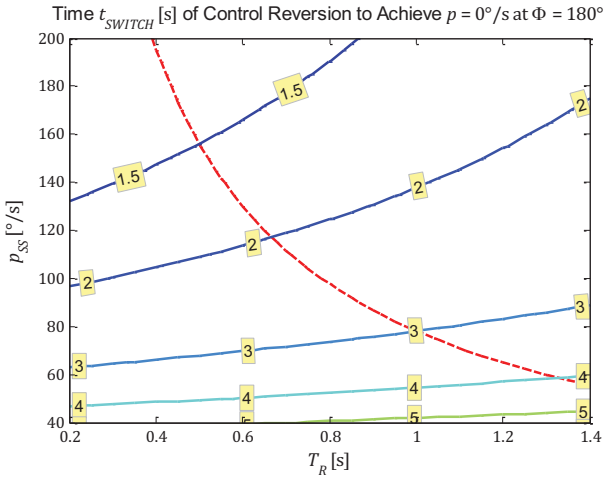

FIGURE 2: Time of control reversion over T_R and p_{SS}.

The validity limit $t_{SWITCH}/T_R = 3$ is indicated by the red dashed line. Hence, valid values for t_{SWITCH} can be found below this line.

In case a configuration to be considered does not lie in the range of valid values, the analysis can be generalized by solving the underlying equations numerically without the assumption of attained p_{SS} at the time of control reversion.

A diagram showing lines of constant $t_{\Phi,STOP}$ over p_{SS} and T_R for $\Phi_{STOP} = 180°$ is given in FIGURE 3.

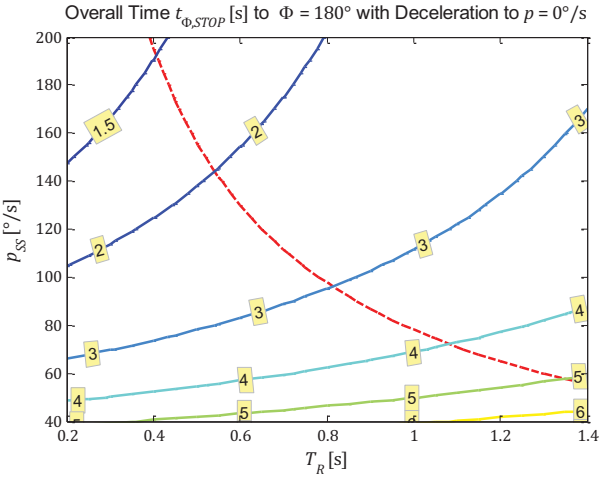

FIGURE 3: Overall rolling time over T_R and p_{SS}.

Although p_{SS} and T_R are typical parameters to describe the roll performance of an aircraft, it is reasonable to provide the lines of constant $t_{\Phi,STOP}$ also in terms of L_p and L_ξ during the design phase.
In order to avoid the specification of a just exemplary value for ξ_0, it is feasible to replace L_ξ by the related roll control moment $\hat{L}_{Ctrl} = L_\xi \xi_0$, i.e. the required body fixed roll control moment normalized with the corresponding moment of inertia I_{xx}^G. The associated diagram with lines of constant $t_{\Phi,STOP}$ is given in FIGURE 4.

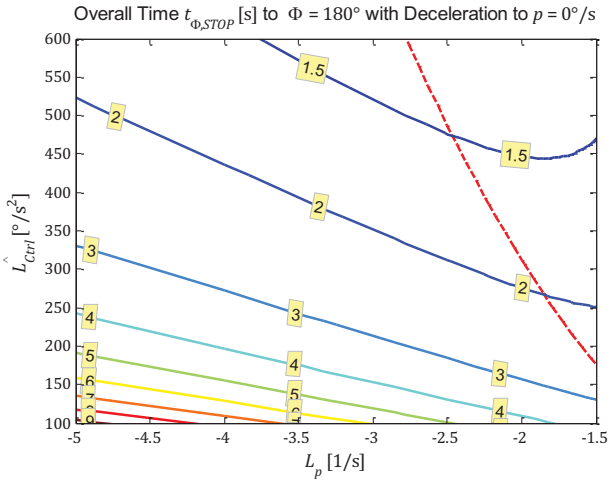

FIGURE 4: Overall rolling time over L_p and $\hat{L}_{Ctrl}$.

Again, the assumption that a steady state roll rate has been reached before the time t_{SWITCH} holds for configurations below the red dashed line.

As accented previously, the conducted analyses have been based on the assumption of an immediate control moment build-up.

Since this assumption typically does not hold, we only provide a lower bound for the needed related roll control moment $\hat{L}_{Ctrl}$. In this sense, configurations that lie below the line of constant $t_{\Phi,STOP} = 2$ s in FIGURE 4 will not be able to satisfy the roll requirement, but on the other hand not necessarily every configuration above the line will satisfy the requirement.

Although the specification of a desired roll performance primarily results in roll control requirements, it is further possible to derive yaw control requirements from the assumption that r and β are constant and equal to zero during the roll. A respective analysis can be found in [1].

4. BASIC STABILIZATION STUDY

As FIGURE 5 reveals, the *SAGITTA Demonstrator* shows (static) lateral-directional instability for angles of attack below 4.5° with the most negative $C_{n,\beta}$ and hence the most severe instability in the vicinity of $\alpha = 0°$.
Hence, controller based stabilization is required and it is essential to assess the stabilization capability already during the configuration design process.

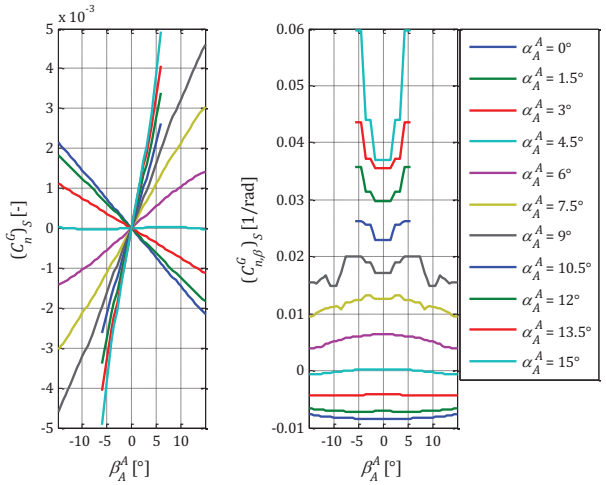

FIGURE 5: C_n and $C_{n,\beta}$ w.r.t. stability axes over β.

Typically, the assessment of the stabilization capability is conducted by means of nonlinear simulation after control effectors and control laws have (preliminary) been specified. This bears the risk of an undesirable high count of design iterations until an adequate trade-off between the degree of instability and the superior design objectives (as performance, low observability, etc.) will be achieved. In contrast to that approach, a basic stabilization study is accomplished for the *SAGITTA Demonstrator* prior to any control effector / control law specification.

The basic stabilization study applies a novel methodology (via transfer of similar pitch-axis considerations [2-4]), balancing the destabilizing moment build-up due to a flow angle disturbance independently, i.e. without respecting controller action, against the counteracting control moment development in terms of a worst case approximation of the real effective moment build-up of a controlled aircraft.
Without a concrete control law defined, it is assumed that the maximum control moment available is commanded step-like after a certain reaction time. Accordingly, the build-up of the control moment in the best case, which is considered in this paper, yields a linear ramp-up to maximum deflection.
Consequently, a control system assessed is rated capable of stabilizing the aircraft if it manages to neutralize the rotation rate resulting from the combination of the unregulated moment build-up and the counteracting control moment potential.

The subsequent sections describe the underlying analysis in more detail.

4.1. Linearized System Dynamics

Considering the lateral motion, the main driver for the destabilization of the aircraft is β via $N_\beta < 0$.
To reduce explicit couplings of the system states involved in the subsequent analysis, it is useful to apply the linearized state space model in notation of the stability-axis frame:

$$\begin{bmatrix} \dot{r}_S \\ \dot{\beta} \\ \dot{p}_S \\ \dot{\Phi} \end{bmatrix} = \begin{bmatrix} N_r & N_\beta & N_p & 0 \\ Y_r - 1 & Y_\beta & Y_p & \frac{g_0}{V_0} \cdot \cos\Theta_0 \\ L_r & L_\beta & L_p & 0 \\ \frac{\sin\gamma_0}{\cos\Theta_0} & 0 & \frac{\cos\gamma_0}{\cos\Theta_0} & 0 \end{bmatrix}_S \begin{bmatrix} r_S \\ \beta \\ p_S \\ \Phi \end{bmatrix} + \begin{bmatrix} N_\xi & N_\zeta \\ Y_\xi & Y_\zeta \\ L_\xi & L_\zeta \\ 0 & 0 \end{bmatrix}_S \begin{bmatrix} \xi \\ \zeta \end{bmatrix} \quad (21)$$

In this notation, the dynamics of yaw rate and angle of sideslip are coupled to the roll rate only via N_p and Y_p which can be omitted both for our UAV without vertical stabilizers.
The influence of the bank angle can also be excluded, provided the flight control system keeps the UAV at a steady bank angle of $\Phi = 0°$ utilizing the roll controls.
For small roll control inputs, it is typically justified to omit the influence of ξ via N_ξ and Y_ξ and hence keeping the bank angle at zero is not considered to affect the dynamics of the yaw rate and the angle of sideslip.
The corresponding reduced system with the yaw controls satisfying $Y_\zeta \approx 0$ is given by:

$$\begin{bmatrix} \dot{r}_S \\ \dot{\beta} \end{bmatrix} = \begin{bmatrix} N_r & N_\beta \\ Y_r - 1 & Y_\beta \end{bmatrix}_S \begin{bmatrix} r_S \\ \beta \end{bmatrix} + \begin{bmatrix} N_\zeta \\ 0 \end{bmatrix}_S \zeta \quad (22)$$

4.2. Response to an Unregulated Disturbance

In this section, the response of the aircraft to a disturbance in angle of sideslip as a result of a cross-wind gust is addressed. We do not yet consider the influence of yaw control trying to stabilize the aircraft.

Without controller action, the homogeneous solution of the system dynamics describes the sideslip build-up and hence, first of all we determine the eigenvalues λ_1 and λ_2 of the system given by Eqn. (22). With these eigenvalues, we can write the development of β over time starting at quasi-steady-state conditions with a disturbance as

$$\begin{aligned} \beta(t) &= Ae^{\lambda_1 t} + Be^{\lambda_2 t} \\ \beta(0) &= \beta_{Dist} \\ \dot{\beta}(0) &= 0 \end{aligned} \quad (23)$$

and with the two constraints, we get

$$\beta(t) = \beta_{Dist}\left(\frac{-\lambda_2}{\lambda_1 - \lambda_2} e^{\lambda_1 t} + \frac{\lambda_1}{\lambda_1 - \lambda_2} e^{\lambda_2 t}\right) \quad (24)$$

For a state space model providing the full dynamics matrix of Eqn. (22), we can right away determine the time history of β using both eigenvalues with Eqn. (24).
However, in the preliminary design phase, it is not always the case that the dynamics matrix is completely available and hence it is reasonable to assess the development of β for the applicability of approximations.
Since λ_1 and λ_2 are for the considered instable system a positive and a negative real eigenvalue, Eqn. (24) poses the summation of an exponentially diverging term and an exponentially decaying term. It is obvious that the diverging term has to be considered, but let us have a more detailed look at the eigenvalues in order to be able to decide on the decaying term. For the subsequent considerations, we imply that λ_2 is the stable eigenvalue.

A well damped system results in a stable eigenvalue far in the left half plane and an unstable eigenvalue significantly closer to zero, i.e. $|\lambda_2| \gg \lambda_1$.
This justifies an approximation without the fast decaying and small contribution of the stable eigenvalue:

$$\frac{\beta(t)}{\beta_{Dist}} = -\frac{\lambda_2}{\lambda_1 - \lambda_2} e^{\lambda_1 t} \tag{25}$$

The corresponding time T_{Double} to double an initial disturbance, a good indicator for the severity of the instability, is then determined to be

$$T_{Double} = \frac{1}{\lambda_1} \ln\left(2\frac{\lambda_1 - \lambda_2}{-\lambda_2}\right) \tag{26}$$

Applying explicitly the property that $|\lambda_2| \gg \lambda_1$, we get a slightly more conservative approximation that gets along with the instable eigenvalue λ_1:

$$\frac{\beta(t)}{\beta_{Dist}} = e^{\lambda_1 t} \tag{27}$$

$$T_{Double} = \frac{1}{\lambda_1} \ln 2 \approx \frac{1}{\lambda_1} \cdot 0.693 \tag{28}$$

A weakly damped system on the other hand results in two eigenvalues almost symmetric to zero, i.e. $\lambda_1 \approx -\lambda_2$.
Assuming actual symmetry, we end up with the following approximation:

$$\frac{\beta(t)}{\beta_{Dist}} = \frac{1}{2}\left(e^{|\lambda| t} + e^{-|\lambda| t}\right) = \cosh(|\lambda| t) \tag{29}$$

The respective time to double the initial disturbance from quasi-steady-state conditions is then determined to be

$$T_{Double} = \frac{1}{|\lambda|} \operatorname{acosh} 2 \approx \frac{1}{|\lambda|} \cdot 1.316 \tag{30}$$

In order to prevent misinterpretations of the effect of damping on the time to double, it shall be mentioned, that T_{Double} is typically smaller for weakly damped systems although $\ln 2 < \operatorname{acosh} 2$. This is an outcome of the effect that $|\lambda|$ of a weakly damped system is significantly bigger than λ_1 of a well damped system with otherwise the same coefficients in the dynamics matrix.

In case of the *SAGITTA Demonstrator*, yaw damping as well as sideslip induced lateral forces are expected to be negligible without vertical surfaces. Hence Eqn. (22) simplifies to

$$\begin{bmatrix} \dot{r}_S \\ \dot{\beta} \end{bmatrix} = \begin{bmatrix} 0 & N_\beta \\ -1 & 0 \end{bmatrix}_S \begin{bmatrix} r_S \\ \beta \end{bmatrix} + \begin{bmatrix} N_\zeta \\ 0 \end{bmatrix}_S \zeta \tag{31}$$

and the characteristic polynomial is given by

$$N(s) = s^2 + N_\beta \tag{32}$$

which results in $|\lambda| = \sqrt{-N_\beta}$ to be applied to Eqn. (29).

For our analysis however, we are not interested in $\beta(t)$, but in the build-up of the unregulated yawing moment.
When focusing on the related yawing moment

$$\widehat{N} = \frac{N_S}{I^G_{zz,S}} = \dot{r}_S \tag{33}$$

we can immediately derive from the state space model in Eqn. (22) that β and r_S contribute to the yawing moment via N_β and N_r respectively.
Thereby it poses a worst case approximation to omit the small contribution of the yaw damping since it would counteract to the destabilizing moment resulting from the build-up of the angle of sideslip.
Consequently, we will consider the following related moment to act on the unregulated aircraft:

$$\widehat{N}_{w/o\ Ctrl}(t) = N_\beta \cdot \beta(t) \tag{34}$$

4.3. Criterion for the Stabilization Capability

For the assessment of the stabilization capability, we include next the application of the control effectors, respectively the resulting moment in our considerations.

As briefly addressed in the introduction of Section 4, a control system is rated capable of stabilizing the aircraft if it manages to neutralize the rotation rate resulting from the combination of the unregulated moment build-up and the counteracting control moment potential.

Written down in equations, it must consequently hold for a finite time $T_{Stab} > 0$ that

$$\int_0^{T_{Stab}} \left(\widehat{N}_{w/o\ Ctrl}(\tau) + \widehat{N}_{Ctrl}(\tau)\right) d\tau = 0 \tag{35}$$

Graphically, this condition is satisfied if the area between the unregulated moment and the negative value of the control moment after the moment equilibrium is equal to the respective area in advance of the equilibrium.
In case the area after the equilibrium is larger than the area in advance, the control system is able to bring the disturbed angle back to its initial condition.

The principle of this approach is depicted in FIGURE 6 for two different control systems with an identical reaction time and ramp-up time.

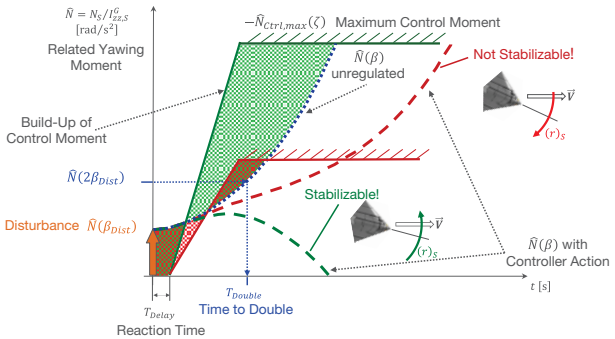

FIGURE 6: Principle of the stabilization capability.

In case of the system depicted in red, the area after the equilibrium is smaller than the area in advance and hence a system with control effectors of these characteristics might not be able to neutralize the yaw rate.
The system is likely to be not stabilizable.

On the other hand, the system depicted in green with a higher maximum control moment is even capable of bringing the angle of sideslip back to zero.
The system is hence stabilizable.

4.4. Stabilization Capability Assessment

In the first step of the stabilization capability assessment, the time history of $\widehat{N}_{w/o\ Ctrl}(t)$ has to be determined for the instability under trim conditions or the worst case instability with all initial disturbances that shall be covered.
Since Eqn. (34) is linear in $\beta(t)$ and Eqn. (24) respectively Eqn. (29) is linear in β_{Dist}, it is sufficient for this purpose to determine $\widehat{N}_{w/o\ Ctrl}(t)/\beta_{Dist}$ once and to scale it for all initial disturbances with the desired β_{Dist} afterwards.

Next, the time history of the related control moment is determined for control systems characterized by:

$$T_{Delay}$$

Since the time instance of a disturbance in β cannot be predicted, there is a certain time delay or reaction time between the disturbance and the time instance when the control effectors get the command to provide a control moment for stabilization of the aircraft.
The higher the delay, the harder it is to make up for the built-up rotation rate.

$$T_{Ramp-Up}$$

The control effectors are limited in their dynamics.
In early design stages without detailed knowledge of these dynamics, it is suitable to assume a linear ramp-up from zero control moment to the maximum attainable control moment within the time $T_{Ramp-Up}$.
With slow control effectors, it might not be possible to stabilize the aircraft despite reasonable time delays and reasonable maximum control moments.

$$\widehat{N}_{Ctrl,max}$$

High initial disturbances can only be stabilized with sufficiently effective control effectors. Even a step-like application of the maximum control moment without any delays will not result in the stabilization of the aircraft if the control moment stays below the moment corresponding to the initial disturbance.
The control effectiveness directly affects the maximum applicable control moment as well as the control moment build-up rate and hence little control effectiveness is exceptional disadvantageous for the aircraft's stabilization capability.

Finally, the integration according to Eqn. (35) is applied numerically e.g. till $3 \cdot T_{Double}$ for all combinations of the related unregulated moment and the related control moment. The result is checked afterwards for a zero crossing at $t > 0$, which indicates that the rotation rate can be neutralized within the considered timeframe.
For each controls set, the maximum and hence limiting initial disturbance that could be stabilized is stored and later on visualized.

For a complete assessment of the stabilization capability, the analysis has to be applied like the trim curve analysis over different velocities, heights and fuel masses.

Further, it should be applied to the instability under trim conditions as well as the worst case instability in order to be able to identify possible savings of control system characteristics. It might for example be reasonable to apply limitations to the maneuvering envelope if the worst case instability is significantly more demanding than the instability in all relevant trim points.

In the following, the assessment is demonstrated exemplary at $120\ \mathrm{m/s}$ in a height of $500\ \mathrm{m}$ with $20\ \mathrm{kg}$ of fuel for the worst case instability, i.e. $C_{n,\beta} \approx -0.008$ at an angle of attack of zero without yaw damping.

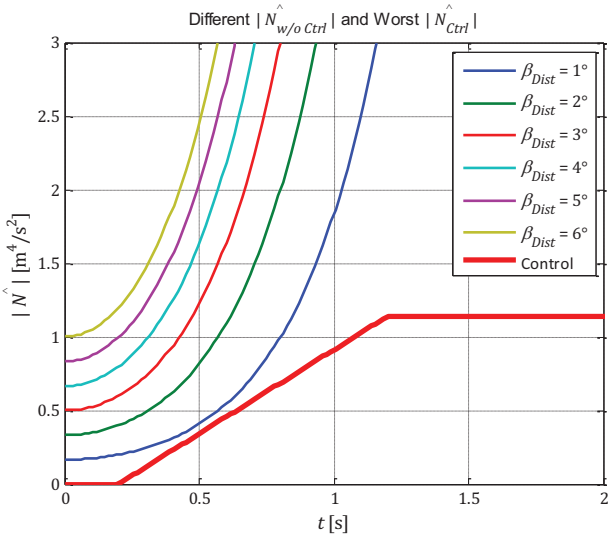

FIGURE 7: $\widehat{N}$ in cross-wind.

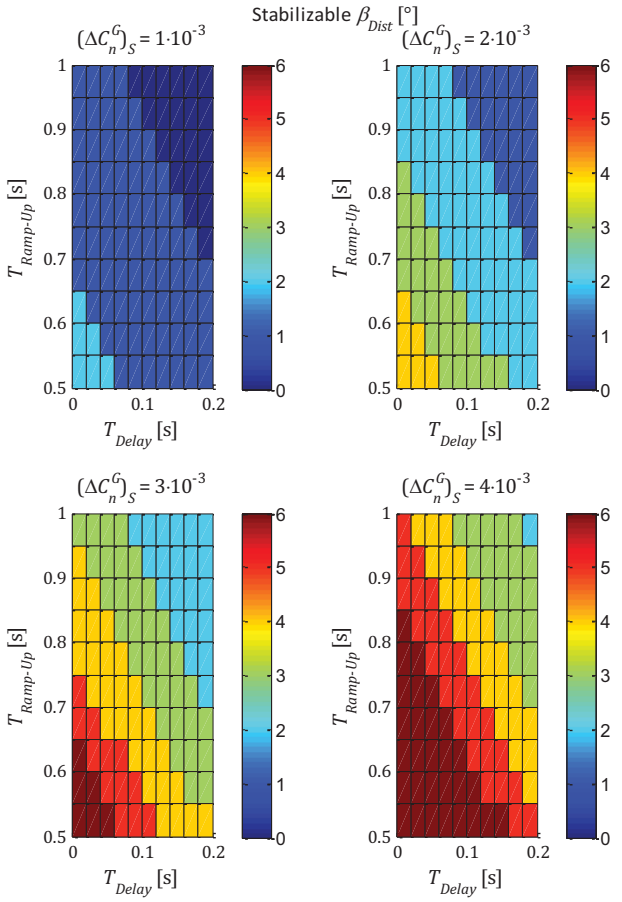

FIGURE 8: Stabilizable β_{Dist} in cross-wind.

It is easy to see from FIGURE 7, that the worst control system applied in the assessment is not capable of stabilizing any of the evaluated disturbances.

More detail on the stabilization capability of the different combinations of the control system's parameters can be found in FIGURE 8, where the color code represents the initial disturbance β_{Dist} that can at least be handled by a given combination of the parameters.
As one can notice, T_{Delay} and $T_{Ramp-Up}$ have a significant influence on the capability to stabilize the UAV although a minimum value for ΔC_n is required.
With $\Delta C_n = 1 \cdot 10^{-3}$ and a fast reaction on the disturbance for example, it is possible to stabilize a $2°$ disturbance which has to be rated not stabilizable for a control system with a doubled control effectiveness but slow reaction.

A suitable control system has to be able to stabilize in every evaluated flight condition at least an initial disturbance equal to the angle of sideslip that corresponds for the evaluated airspeed to the limited cross-wind.
From this point of view, it is useful to provide FIGURE 8 also with a color code reduced to the binary statement *Stabilizable* or *Not Stabilizable* for a quick evaluation.
Within the set of suitable control systems, the full color code indicating the stabilizable β_{Dist} is still important since it enables the engineer to trade the three parameters T_{Delay}, $T_{Ramp-Up}$ and ΔC_n off against each other.

5. CONCLUSION

The specifics of the modelling for flight dynamics analysis in early design stages have been addressed briefly.
Subsequently, the basic idea of applying trim curve analysis for the derivation of control requirements using simplified models has been imparted.
Next, the derivation of configuration demands from mission related requirements has been demonstrated in detail for the example of the roll performance. Here, a lower bound for the roll control effectiveness depending on the configuration's roll damping has been derived.
Finally, a basic stabilization study conservatively assessing the effect of time delays as well as the dynamics and the effectiveness of yaw control effectors on the capability to stabilize a lateral-directional unstable configuration has been presented.
Both, the lower bound for the roll control effectiveness as well as the conservative yaw control requirements do not represent a specification of ideal control effectors. Instead they provide, based on a manageable set of inputs, a starting point for the control effector specification and hence support to reduce the count of design iterations.

For future work, a demand for further means of deriving control effector dynamics requirements in early design stages exists. This is especially relevant for the dynamics of control effectors not involved in the stabilization of the aircraft. From our point of view, it is most promising to obtain respective requirements from the UAV's mission.
Beyond that, it is intended to further accompany the design process of the *SAGITTA Demonstrator* with the assessment of suggested control effectors and by designing control laws for the flying wing. Amongst others, this will enable an assessment of the conservatism of the initially derived requirements.

Acknowledgements

This paper has been composed with the support of the Technische Universität München – Institute for Advanced Study, funded by the German Excellence Initiative.

References

[1] Geiser M (2011) Modelling, Simulation and Flight Mechanics Analysis of a Low Observability Flying Wing UAV. Diploma Thesis, Institute of Flight System Dynamics, Technische Universität München, Munich, Germany
[2] Mangold P (1990) Integration of Handling Quality Aspects in the Aerodynamic Design of Modern Unstable Fighters. AGARD Flight Mechanics Panel Symposium on Flying Qualities, Quebec City, Canada
[3] Mangold P (1992) Flugmechanisch Basisauslegung moderner Kampfflugzeuge. Manuskrip-Nr. 3, Carl Cranz Gesellschaft e.V., Oberpfaffenhofen, Germany
[4] Heller M (2011) Flugdynamische Herausforderungen hochgradig-reglergestützter Konfigurationen. Lecture, Institute of Flight System Dynamics, Technische Universität München, Munich, Germany